Fermi-Bose Mixtures and BCS-BEC Crossover in High-T$_c$ Superconductors

Maxim Yu. Kagan [1,2,*] and **Antonio Bianconi** [3,4,5]

[1] National Research University "Higher School of Economics", ul. Myasnitskaya 20, 101000 Moscow, Russia
[2] P.L. Kapitza Institute for Physical Problems, Russian Academy of Sciences, ul. Kosygina 2, 119334 Moscow, Russia
[3] Rome International Center for Materials Science, Superstripes, via dei Sabelli 119A, 00185 Roma, Italy; antonio.bianconi@ricmass.eu
[4] Institute of Crystallography, CNR, Via Salaria Km 29.300, Monterotondo, I-00015 Roma, Italy
[5] National Research Nuclear University MEPhI (Moscow Engineering Physics Institute), 115409 Moscow, Russia
[*] Correspondence: kagan@kapitza.ras.ru or mkagan@hse.ru

Abstract: In this review article we consider theoretically and give experimental support to the models of the Fermi-Bose mixtures and the BCS-BEC (Bardeen Cooper Schrieffer–Bose Einstein) crossover compared with the strong-coupling approach, which can serve as the cornerstones on the way from high-temperature to room-temperature superconductivity in pressurized metallic hydrides. We discuss some key theoretical ideas and mechanisms proposed for unconventional superconductors (cuprates, pnictides, chalcogenides, bismuthates, diborides, heavy-fermions, organics, bilayer graphene, twisted graphene, oxide hetero-structures), superfluids and balanced or imbalanced ultracold Fermi gases in magnetic traps. We build a bridge between unconventional superconductors and recently discovered pressurized hydrides superconductors H$_3$S and LaH$_{10}$ with the critical temperature close to room temperature. We discuss systems with a line of nodal Dirac points close to the Fermi surface and superconducting shape resonances, and hyperbolic superconducting networks which are very important for the development of novel topological superconductors, for the energetics, for the applications in nano-electronics and quantum computations.

1. Introduction

The seminal discovery in 1986 of high-T_C superconductivity at 36 K in a doped cuprate perovskite La$_{2-x}$Ba$_x$CuO$_4$ by Karl and Johannes in IBM Zurich [1,2] determined the shift of research for room-temperature superconductors from metallic alloys to complex perovskites. In the first 10 years the critical temperature of gradually increased from 36 K in lanthanum family of superconducting cuprate perovskites till 90 K in yttrium family YBa$_2$Cu$_3$O$_{7-\delta}$ and finally reaching 160 K in HgBa$_2$Ca$_2$Cu$_3$O$_8$ under the applied pressure of P = 350 GPa. This extraordinary progress promised a technological revolution in electronics, and energetics and provided the driving force for tremendous progress in the development of many body theories for condensed matter physics, inorganic chemistry and material science. Today we see the growing interest on quantum complex materials. The conventional superconductivity in low-temperature superconductors is described by the BCS weak coupling theory in a homogeneous metal with Cooper pairing on a large Fermi surface with high Fermi

energy. The unconventional high temperature superconductors are characterized by the breakdown of the standard BCS approximations:

1) A single electronic component;
2) High electron density and high Fermi energy E_F;
3) Low values of the ratio ω_0/E_F between the energy cut off of the attractive interaction ω_0 and the Fermi energy;
4) Large Fermi surface and high Fermi momentum k_F;
5) Superconducting energy gap much smaller than the Fermi energy $\Delta << E_F$;
6) Large ratio between the coherence length ξ_0 and the average distance between electrons.

Soon after the discovery of Müller, Anderson and Schrieffer advanced different unconventional mechanisms for high temperature superconductivity (see e.g., References [3–5]). Many fruitful ideas were introduced in the first years of HTSC by the leading theorists in USA, Europe, Japan and worldwide (see e.g., References [6–16]). One of the authors of the present review was very active in unconventional mechanisms focusing on the low-density electron systems [17–24] based on the generalization of Kohn–Luttinger ideas [25,26] in purely repulsive Fermi systems. In the framework of the Fermi gas model with hard-core repulsion [27], repulsive-U Hubbard model [28] and the Shubin–Vonsovsky model [29,30] on different type of 3D and 2D lattices during last 30 years of intensive research we predicted p-, d-, f- and anomalous s-wave pairing in various materials, such as the idealized and bilayer graphene (see Figure 1), superconducting pnictides and organic superconductors and superfluid ^{3}He.
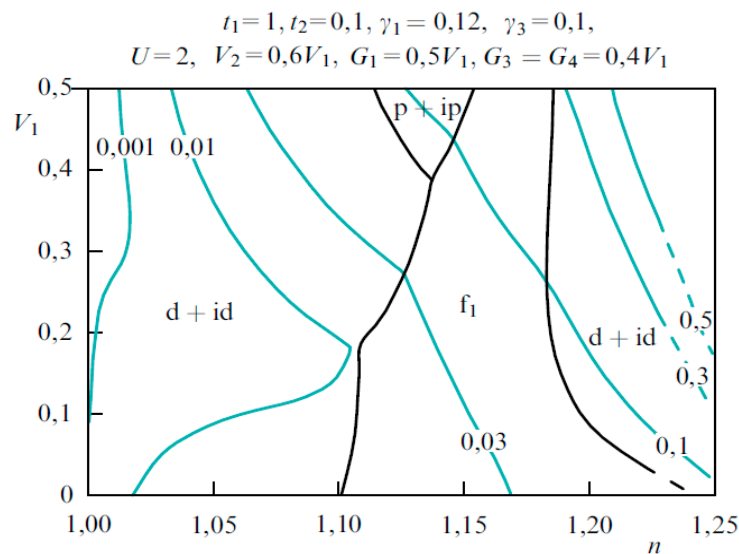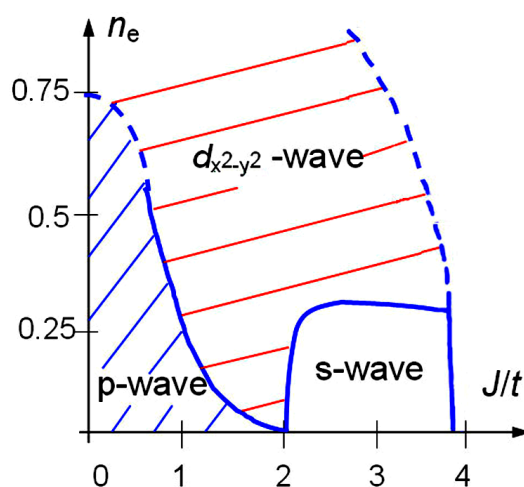

Figure 1. Phase diagram of superconducting state in the AB structure of the bilayer graphene [21] shown as a function of the variables $n − V_1$, where $1 < n < 1.25$ is the carriers density, t_1, t_2 and γ_1, γ_2 are intralayer and interlayer hoppings, U is onsite Hubbard repulsion, V_1, V_2 and G_1, G_3, G_4 are intralayer and interlayer Coulomb repulsions. The leading SC instabilities correspond to chiral $p + ip$, $d + id$ and f_1-pairing. For all the points on the same thin line the value of the coupling constant $|\lambda| = 1/\ln(E_F/T_C)$ is constant.

It has been shown that the critical temperature of the superconducting transition can be substantially increased at low densities by considering spin-polarization or the two-band superconductivity scenario [31–33]. These results proved to be very important for related systems as in polarized ^{3}He-^{4}He mixtures, imbalanced Fermi-gas in the magnetic trap, as well as for heavy fermion superconductors and other mixed valence systems described by the two-band Hubbard model with one narrow band [34–37]. Together with T.M. Rice we also considered a superconductivity

scenario in 2D t-J model at low and intermediate electron density [38,39] with van der Waals interaction which corresponds to strong onsite Hubbard repulsion and weak intersite antiferromagnetic (AFM) attraction. The phase-diagram of this model presented in Figure 2 shows regions of superconducting phases with different pairing symmetry: P-wave, s-wave and $d_{x^2-y^2}$-pairing. For small values of J/t the phase-diagram of the 2D t-J model becomes equivalent to the phase-diagram of the 2D Hubbard model and according to the results [17–19] is unstable at low electron densities towards p-wave superconductivity of the Kohn-Luttinger [25] type. At large values of $J/t \geq 2$ (which usually are not realized in cuprates) the system becomes unstable towards extended s-wave pairing. For the set electron densities (optimal doping) and the values of $J/t \sim 1/2$ we get the critical temperature of the d-wave pairing typical for high-T_C,

$$T_C \sim E_F \exp\left(-\frac{\pi t}{2 J n_e^2}\right) \sim 100K. \tag{1}$$

Figure 2. The phase-diagram of the superconducting state of 2D t-J model [38,39].

This result was generalized by Plakida et al. [40,41] on the opposite case of small hole densities $x = (1 - n_{el}) \ll 1$ using the diagrammatic technique of the Hubbard operators for the pairing of two spin polarons. The same order of magnitude T_C: 100 K for the critical temperature can be obtained for the d-wave pairing in the Shubin-Vonsovsky model in the intermediate coupling case for the set of parameters $U \approx 3t, n_{el} \approx 0.9$ [20,21,24] on the 2D square lattice.

We would like to summarize here both the early stage [42–53] and recent [54–58] theoretical results of the Russian research school in high-T_C investigations.

The proposed mechanisms of superconductivity in high-T_C cuprates range from BCS scenarios involving electron-phonon or electron-electron interactions, with extended pairs [59] or BEC scenarios with local pairs [60,61], with condensates of s-wave or d-wave [4,6,8,12] in models of the normal phase described by Landau Fermi liquid [62,63], Luttinger [64] or marginal [13] Fermi liquid (correspondingly with spinons and holons instead of fermionic quasiparticles), spin-charge separation [3,6,12,64,65] or spin-charge confinement [11,65], with the presence of pseudogap [66] in underdoped state, including interplay between superconductivity and antiferromagnetism [67], formation of stripes [14], the role of the second layer and the c-axis plasmon mode [15] have been the subject of an intensive debate.

In 2015 following theoretical predictions [68,69] for high Tc in the high-pressure metallic phase H_3S the record [70] for the superconducting temperature of 203 K was reached. The authors of the experimental breakthrough claimed that the discovered superconductivity could be explained by the conventional strong-coupling version of the BCS theory [71] constructed by Migdal and Eliashberg [72,73] used to predict the high Tc phase in the dirty limit [69,70]. It was rapidly shown that by changing the pressure to reach the maximum critical temperature the chemical potential in

H_3S is driven to an electronic topological transition known as a Lifshitz transition for the appearing of a new piece of a Fermi surface [74,75]. In this regime the Migdal approximation breakdown [76] and it is not possible to apply the BCS theory to explain the emergence of high temperature superconductivity. It has been shown that the emergence of high temperature superconductivity in a multiband scenario near a Lifshitz transition has been described by numerical solution of Bogoliubov equations [77] and can be qualitatively predicted in the limit of a steep–flat scenario [78] where the energy dispersion of the appearing band is pushed down to zero as for the case of an infinite effective mass for strong correlated localized states [79]. An essential point of this proposed scenario for the emergence of room temperature superconductivity is the theoretical demonstration that the Lifshitz transition for the appearing of a strongly correlated band is not of 2,5 order, but becomes of first order with appearing of a frustrated phase separation [78], interface superconducting [80] and a hyperbolic space of filamentary pathways in two dimensional systems like it was observed in cuprate perovskite superconductors at optimal doping [81].

Recent papers on pressurized hydrides under high pressure support early papers [82] and support the multigap superconducting scenario in the proximity of a Lifshitz transition [83].

Quite recently two experimental groups [84,85] reported a discovery of even higher critical temperatures T_C: (250–260) K in lanthanum superconducting hydrides $LaH_{10\pm x}$ at high pressures P: (170–190) GPa. In this compound, according to the Density Functional Theory (DFT), the host atom of La is at the center of the cage formed by hydrogen atoms. Moreover, the authors of [86] on the basis of numerical calculations predict the topological Dirac nodal line in LaH_{10} near the Fermi energy E_F. Note that room critical temperatures (RTSC) of the order of 300 K or higher in metallic hydrogen for very high pressures P: (170–190) Mbar and in hydrogen dominant metallic alloys (at smaller pressures) were predicted by Ashcroft [87,88]. The large values of T_C in Ashcroft estimates were facilitated by the high phonon frequencies governed by the light mass of hydrogen ions.

It is important to note that the profound numerical calculations of the local minima of the optimal crystalline structure performed by Brovman, Yu. Kagan and Kholas [89,90] show the regions of 3D isotropic phase, quasi-2D planar phase and quasi-1D filamentary phase on the P–T phase-diagram of metallic hydrogen. In particular, they predict at relatively low pressures and $T = 0$ a strongly anisotropic phase with the proton filaments embedded in electron liquid. The filaments can move almost freely relative to each other in the longitudinal direction similar to vortices in superfluid ^{4}He [91] (where we have a vortex crystal in the perpendicular direction to the vortex lines, and a free superfluid in the parallel direction to the vortex lines). In the same time the filaments form a rigid triangular lattice in the direction perpendicular to them which resembles Abrikosov vortex lattice in type-II superconductors [92]. Similarly, in the planar phase the hydrogen layers can move almost freely relative to each other similarly to the smectic liquid crystals or graphite layers.

2. Superconductivity in the Fermi-Bose Mixture Model—Theoretical Considerations

The authors stress that the light mass of hydrogen ions H^+ not only guarantees the high values of Debye frequency, but also leads to a large kinetic energy of zero-vibrations and thus to a large value of De Boer parameter measuring the ratio of kinetic delocalization energy and potential energy and responsible for the quantumness of the system [39,93]. This fact brings a highly mobile ionic subsystem in metallic hydrogen (which resembles superionic crystal, but at low temperatures in our case) close to the limit of the quantum crystal [39,93]. Note that high mobility of filaments or layers can promote also rather large values of Lindeman parameter (Lindeman number [39,93]). It measures the ratio of the root mean square of the displacement of ion to the interionic distance in metallic hydrogen or in hydrogen dominant alloys and shows that our system is close to the quantum melting limit. In principle, according to the ideas of Andreev, Lifshitz the ionic lattice of the quantum crystal can become superfluid at low temperatures (due for example to a flow of vacancies or other defects relative to the lattice, or due to delocalization of filaments themselves which can form the macroscopic wave function). This phenomenon is nowadays called a supersolidity of the quantum

crystal [94]. Experimental indications on available today scenarios for quantum supersolid are discussed by Bianconi group in Reference [81]. The experimental support for filamentary supersolids can be found in References [76,79] having in mind not only "new" hydrogen dominant superconductors, but also the "old" cuprate perovskites.

In analogy with neutron stars we can describe the ionic subsystem on the language of biproton superfluidity which coexists with the BCS Eliashberg superconductivity of the electron subsystem (probably modified on the frequency dependence of effective mass and nonconstant density of states [95]).

These qualitative considerations pressed the authors to consider the superconductivity in metallic hydrogen on the level of Fermi-Fermi mixture [96] of protons and electrons (as in plasma physics or in the two components model with one very narrow band [36,37]) or on the level of Fermi-Bose mixture of Cooper pairs and protons or even of Bose-Bose mixture [97] of Cooper pairs and biprotons. Note that the ideas of Fermi-Bose mixture were very fruitful in low temperature physics describing the search for fermionic (BCS) superfluidity in dilute 3D and 2D solutions of ^{3}He in superfluid ^{4}He [34,98–100], as well as ^{6}Li-^{7}Li or ^{40}K-^{87}Rb mixtures of ultracold atoms [101–103] in restricted geometry of magnetic and dipole traps or on the optical lattices.

Note that in ultracold Fermi gases there is a very effective way to change the magnitude and the sign of the interaction (more precisely of the s-wave scattering length) between the atoms. This can be done in the resonance magnetic field, in the regime of Feshbach resonance [104] which is important for the physics of BCS-BEC crossover in quantum gases. The Fermi-Bose mixture model corresponds to the two-channel description of the Feshbach resonance [105]. Here we have the attractive Majorana exchange term which transforms the (extended) Cooper pair consisting of two fermions in one channel into a real boson (a local pair or dimer) in the other channel.

In the physics of superconductors, the model of Fermi-Bose mixture was firstly proposed by Lee et al. [106] and Micnas et al. [107]. for superconducting cuprates. In this model the Majorana exchange term which transforms the Cooper pair in a boson, is present. Later on, Larkin, Geshkenbein and Ioffe [108] phenomenologically advanced this model on the level of Ginzburg–Landau theory [109] for 2D electron system described by Hubbard type models close to van Hove singularities and for two-leg ladder systems [110].

Note that the Fermi-Bose mixture model with an additional requirement of the spatial separation of Fermion and Boson component captures thermodynamic and transport properties, as well as a lot of essential features on the phase diagram of superconducting bismuth oxides $Ba_{1-x}K_xBiO_3$ [111,112]. The local pairs are formed in these materials in BiO_6 clusters (see Figure 3). The critical temperature $T_c \sim 36$ K corresponds here to the coherent tunneling of local pairs between neighboring Bose clusters through the effective barriers formed by Fermi clusters.

The generic Hamiltonian of the Fermi-Bose mixture typically has the form,

$$H = H_F + H_B + H_{BF}, \tag{2}$$

where fermionic and bosonic parts H_F, H_B are Hubbard like and interaction term has a form resembling electron-phonon interaction.

In the second order of perturbation theory an interaction term also becomes Hubbard-like [102]

$$H_{FB} = U_{FB}\sum n_{iF}n_{iB}, \tag{3}$$

and depending upon the sign of U_{FB} describes either Fermi-Bose mixture with repulsion [34] or with attraction [103] between fermions and bosons.
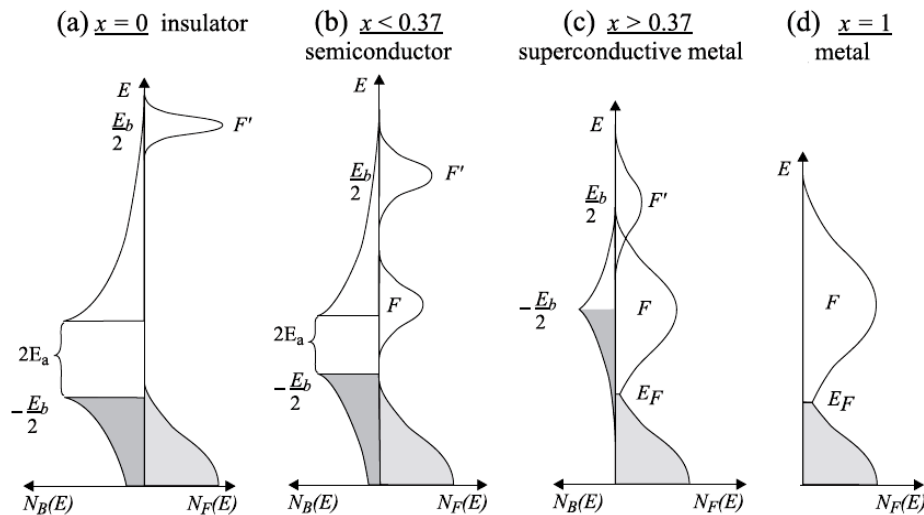
Figure 3. Interplay between Fermi and Bose subsystems in superconducting $Ba_{1-x}K_xBiO_3$ [21,111,112]: (**a**) insulator, $x = 0$; (**b**) superconductor, $x < 0.37$; (**c**) superconductive metal, $x > 0.37$; (**d**) metal, $x = 1$.

The Fermi-Bose mixture of spinons and holons interacting via a strong confinement potential [8,65] created by an AFM string [113,114] was considered in Reference [115] for the underdoped high T_C cuprates. The main idea was to describe the superconducting pairing in the strongly underdoped region of the t-J model on the language of the BCS-BEC crossover for the pairing in the d-wave channel of two spin polarons (two composite holes or two strings), where the critical temperature in the BCS phase is governed by (Equation (1)) and its spin-polaronic generalization [40,41]. The crossover, however, is probably not smooth, containing the quantum critical point (QCP) or even intermediate phases in between BCS and BEC phase [115].

Note that non-phonon mechanisms of superconductivity can easily explain superconductivity with the critical temperature of the order of of $T_c = 100$ K, typical for cuprate perovskites. However, to get T_C: (250–260) K typical for metallic hydrogen alloys another type of models, such as Fermi-Bose mixture model or the Fano shape resonance mechanism with exchange interaction between a first BCS and a second condensate in the BCS-BEC crossover regime model is needed.

3. The 3D and 2D Models of BCS-BEC Crossover

Note that to some extent the Femi-Bose mixture model naturally appears in the most difficult intermediate part of the phase diagram for the BCS-BEC crossover [21,116] between extended Cooper pairs (dilute BEC regime) and local pairs (or bipolarons [117,118]) which correspond to the weakly repulsive Bogoliubov gas [119] of composed bosons (see Figure 4).
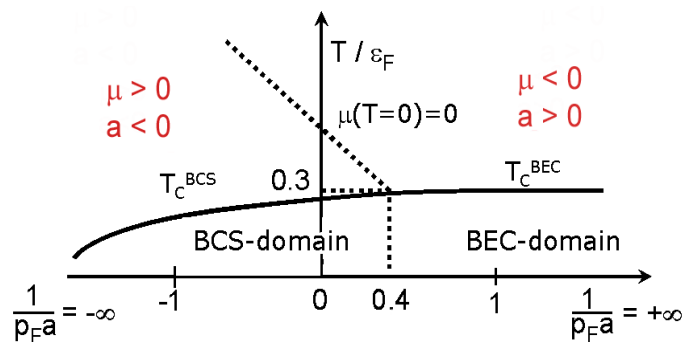
Figure 4. The typical phase-diagram of BCS-BEC crossover between extended Cooper pairs and local pairs in the 3D Fermi gas [21,116].

Namely, for the dilute Bose gas, we have two distinct temperatures $T*$ which corresponds to the formation of local pairs and T_C of their Bose-condensation. For intermediate temperatures:

$$T_C \ll T \ll T*, \tag{4}$$

where the critical temperature of BEC,

$$T_C = 3.31 \frac{(n/2)^{2/3}}{2m}[1 + 1.3a_{2-2}n^{1/3}] \approx 0.2E_F, \tag{5}$$

is mostly governed by Einstein formula [120] for the number of pairs density $n_B = n/2$ and the mass of the pair $m_B = 2m$. However, there are nontrivial corrections to Einstein results connected with weakly repulsive interaction between the local pairs (between the dimers) [121]. This interaction is defined by the dimer-dimer scattering length $a_{2-2} = 0.6|a| > 0$ [122,123], where a is an s-wave scattering length for particle-particle interaction. In the same time the crossover (Saha) temperature [21,116,124].

$$T* \sim \frac{|E_b|}{3/2\ln(\frac{|E_b|}{E_F})}, \tag{6}$$

where $|E_b| = 1/ma^2$ is an absolute value of the binding energy of a local pair, $E_F = \frac{p_F^2}{2m}$ is the Fermi energy, p_F is Fermi momentum.

Note that in the 2D case we have a similar estimate for the Saha temperature [124–126],

$$T* \sim \frac{|E_b|}{\ln(\frac{|E_b|}{E_F})}. \tag{7}$$

In the same time the BEC critical temperature is given by Fisher-Hohenberg theory [127] for weakly repulsive 2D Bose gas. According to Reference [127]

$$T_C \sim \frac{E_F}{4\ln(1/f_{2-2})}, \tag{8}$$

where $f_{2-2} \sim 1/\ln(1.6|E_b|/E_F)$ [128] describes the repulsive interaction between the dimers in 2D.

For the intermediate temperatures in (Equation (4)) we have a new state of matter, namely the normal (non-superconducting) metal. According to References [116,126] it has very peculiar transport and thermodynamic properties with a resistivity behaving in semiconducting fashion $R \propto \sqrt{T}$.

In the same time in the intermediate coupling case (for the values of the gas parameter $1 \leq ap_F \leq 3$ [21]) the binding energy of the pair $|E_b|$ becomes comparable with the Fermi-energy E_F. When we increase the density, we finally reach the limit $|E_b| \leq 2E_F$, and the local pairs start to touch each other. As a result, some of the local pairs are crushed and (in the framework of e.g., 3D Fermi gas with attraction or attractive-U Hubbard model) we have a Fermi-Bose mixture of paired and unpaired electrons already at low temperatures.

With some precaution we can also describe the low temperature phase in case of intermediate coupling on the language of the Bose-Bose mixture of two coexisting Bose condensates one in the limit of extended pairs and a second one in the limit of almost local pairs.

4. Fano Resonances in Multigap BCS-BEC Superconductivity in the Regime of the BCS-BEC Crossover at Lifshitz Transitions

Major schools of unconventional mechanisms for high temperature superconductivity have been based on the assumption of a "single electronic component" forming the superconducting condensate. The resonant valence bond theory proposed the condensation of preformed electronic

pairs in a doped Mott insulator [3], the spin fluctuation theory proposed the pairing mediated by spin fluctuations in a strongly correlated metal [4]. The conventional BCS theory usually considers a single electronic component, both in the weak coupling, as well as in the strong coupling limit. In these standard theories the superconductor is formed by a single quantum condensate. In order to apply the BCS theory to a large variety of superconductors the complex band structure of metals with multiple Fermi surfaces is reduced to a single band theory using the "dirty limit approximation". However, these "standard theories" have been falsified by the results of material science which has found high temperature superconductivity not in simple elemental metals which can be reduced to a single electronic component in a single Fermi surface, but in complex multi-components materials with coexistence of multiple distinguishable electronic components with different orbital symmetries at the Fermi level with multiple different Fermi surfaces going from A15 intermetallics, doped cuprate perovskites, diborides, iron based superconductors, pressurized hydrides. In these systems, different pairs in multiple portions of the Fermi surfaces condense in a single macroscopic coherent quantum state formed by multiple superconducting quantum condensates with different symmetries. While "exchange interaction" between quantum condensates is not considered and neglected in standard theories of superconductivity it becomes a key ingredient in multigap superconductors. The role of exchange interaction in the formation of a quantum heterogeneous matter made of different components was first faced in quantum mechanics in theories proposed to explain the formation of nuclear matter made by protons and neutrons.

The attractive exchange interaction between bosonic pairs of protons and bosonic pairs of neutrons in Quantum Mechanics was proposed in 1933 by Majorana [129,130] after Heisenberg proposed the well-known repulsive exchange interaction [131,132] between fermionic particles. Majorana demonstrated that symmetry played a vital role in bosonic or fermionic systems. In fact, his force and the one of Heisenberg made very different predictions because of their different symmetry properties. The Majorana exchange interaction opened the road map for both the interaction boson model [133] and the interaction boson fermion model [134], and today it is at the base of the research to extract simplicity in complexity applied to a large spectrum of systems where the focus of the research is to identify the dynamical complex symmetry [135], as shown in Figure 5, for the triangular hyperbolic tiling, and it was extended to the case of high temperature superconductors with multiple gaps [136] and in molecular systems. It is now clear that more complex is the system, the more important is to search for its symmetry as for example in the *vibron model* described by the so-called(4)u algebra and in the *electron-vibron model* described by even more complicated superalgebra (4/)u1 [135].
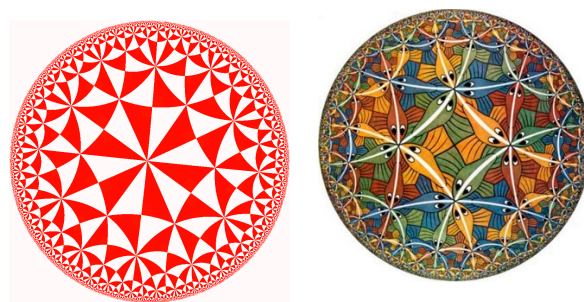

Figure 5. Tessellation of the hyperbolic Poincare' plane: Showing the (6,4,2) triangular hyperbolic tiling (**left side**) that inspired the Escher *Circle limit III* pantin*g* (**right side**) (From *M.C. Escher, Circle Limit III, 1959*). from Wikipedia https://en.wikipedia.org/wiki/Circle_Limit_IIICC BY-SA license: http://creativecommons.org/licenses/by-sa/3.0/.

Fano introduced the configuration interaction between a closed channel and an open scattering channel in Quantum Mechanics in his famous paper published by Nuovo Cimento in 1935 [137]. He expanded and improved his theory in the 1961 Physical Review paper [138]. The idea of the exchange interaction between pairs formed in the cloud of fermionic particles (which he

called "pions") and a localized boson, an extension of Fano resonance, was developed in the quantum field theory of many body systems by Tomonaga [139]. The Fano resonances have been classified as a "*Feshbach resonance*" if scattering length of the system in the closed channel is *negative* and it gives a well localized boson pair at negative energy; or as a "*shape resonance*" if the scattering length of the system in the closed channel is positive and it is a *quasi-stationary state* at positive energy degenerate with the continuum [140].

The Bose fermion or Fermi-Bose model for high temperature superconductors is therefore described as the case of *Feshbach resonance* driven by Majorana exchange interaction between bosonic pairs making a BEC condensate with cooper pairs making a BCS condensate [141–143] which is described in the right panel of Figure 6.
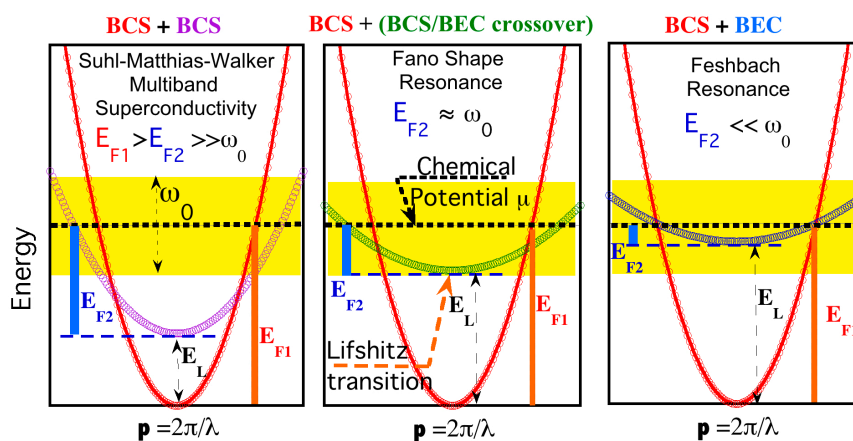
Figure 6. Three typical cases of non-standard superconducting theories of multigap superconductivity where Majorana exchange interaction between two different electronic components with different symmetry plays a key role: (**left**) The case of two BCS condensates in two large Fermi surfaces; (**center**): The case of Fano shape resonance between a first BCS condensate and a second condensate in the BCS/BEC crossover, (**right**): The case of Feshbach resonance between a first BCS condensate and a second condensate in the BEC regime typical of the boson-fermion models.

In 1993 an alternative theoretical scenario for high temperature superconductors driven by Fano resonances of the type called shape resonances [77,80,144–149] was proposed. where the Majorana exchange term is in action between cooper pairs in the BCS condensate and the second condensate of polaronic pairs in the intermediate coupling regime forming a condensate in the BCS-BEC crossover which is described in the central panel of Figure 6. The theoretical proposal was based on compelling experimental evidence collected from the study of the structure of the 91K $Bi_2Sr_2CaCuO_{8+y}$ superconductor that bulk superconductivity emerges in a stack of 2D layers of a strongly correlated electron liquid confined in finite domains of incommensurate modulated aperiodic lattice where two electronic components coexist: A first Fermi liquid and a second polaronic liquid coexisting with a polaronic generalized Wigner charge density wave [144–146].

The "*shape resonance*" driven by Majorana exchange interaction between a first condensate in the BCS-BEC crossover and cooper pairs in a BCS condensate appears by tuning the chemical potential to the electronic topological transition called Lifshitz transition in a correlated interacting low dimensional metal [147–149]. This non-standard and unconventional superconductivity scenario is completely beyond all BCS approximations and it was described theoretically by solving numerically the Bogoliubov anisotropic gaps equations at the same time as the density equation, called Bianconi-Perali-Valletta (BPV) approach [77,80,147–149].

The BPV theory predicts that the critical temperature is a strong function of the physical parameters like strain, doping, pressure, uniaxial pressure, charge density, gate voltage etc. which tune the system near the Lifshitz transition with a strongly anisotropic resonance of the superconducting critical

temperature and the superconducting gap with Fano line-shape not predicted by standard single band theories.

The "shape resonance" superconducting phase in the proximity of two Lifshitz transitions is supported in cuprates by the fact that the maximum critical temperature occurs at optimum doping = 0.16 where the Fermi surface is made of disconnected Fermi arcs in the proximity of two topological electronic transitions. The first one is at 0.21 holes per Cu site where for larger doping a large circular Fermi surface appears and the second for 0.125 holes per Cu site where the Fermi surface shrinks to only four very short Fermi arcs in the diagonal direction with a maximum isotope coefficient [149]. Complexity emerged at the beginning of the XXI century, as the second key universal feature of cuprate superconducting perovskites [150–152]. Three key features of high temperature superconductors were established: (i) Mesoscopic and nanoscale phase separation [150] (see also review article [153]), (ii) multiple electronic components in the normal metallic phase [151], (iii) the key role of anisotropic lattice strain driving the complexity [152] and coexisting multiple superconducting gaps spatially distributed at nanoscale. The phase separation scenario with spin, charge, lattice nanoscale puddles with the proliferation of interface filamentary space was called a *Superstripes* scenario i.e., a supersolid with a specific symmetry [154] (see also Figure 6 for illustration).

The BPV theory was presented at the first Stripes conference in 1996, before the discovery of superfluid condensation of ultracold bosonic gases in 1998 and the superfluid condensation of fermionic gasses in 2002 driven by the Feshbach resonance mechanism. At the Rome Stripes conference in 2000, the key role of anisotropic misfit-strain and the strain-doping-temperature phase diagram in the proximity of a Lifshitz transition have been presented. A few months, later in December 2000, the superconducting properties of MgB_2, a binary metallic non-magnetic system, known for fifty years, have been measured in Japan by Akimitsu. MgB_2 was a layered system not expected to be a BCS superconductor, showing the record of $T_c = 40$ K for a binary alloy. It was rapidly claimed that it was a clear case of superconductivity driven by a Fano shape resonance near a Lifshitz transition for the appearing of a new spot of a sigma Fermi surface with the key role of a large amplitude zero-point motion at low temperature [155,156]. The BPV model predicted, and provided, the first published explanation of the high critical temperature in diborides. This is where the misfit strain, and doping, moves the chemical potential in the $Al_{1-x} Mg_x B_2$ and $Sc_{1-x} Mg_x B_2$ below the Lifshitz transition for the appearing the sigma Fermi surface for x > 0.5 [155]. It was the first case of a verified prediction of the BPV theory in a completely different system [147–149]. The second key feature, *nanoscale phase separation*, was found by doping MgB_2 with aluminum or scandium substitution for Mg [157] which shifts the chemical potential toward the Lifshitz transition.

The second case of a different practical realization of the Fano shape resonance high temperature superconducting was reported in 2008 with the discovery of iron based superconductors [158–161] which are stacks of superconducting iron layers which show a strain doping phase diagram with maximum critical temperature in proximity of a Lifshitz transition [158–161].

After 2008 new microscopes using focused synchrotron radiation have shown a ubiquitous presence of nanoscale phase separation in high temperature superconductors in cuprates [81,162–164] and in iron based superconductors [165–168] providing the theoretical prediction that nanoscale phase separation is a universal feature of systems showing Fano shape resonances in proximity of a Lifshitz transition [169–171] in the *superstripes* scenario [154] which is called by some authors with the generic name of intertwined or nematic phase. The theoretical efforts to understand the nanoscale phase separation in high temperature superconductors has pointed out the complexity of possible variable tilting of local structure in perovskites [170], the mixing of boson and fermions in the complex symmetry [171,172], the role of anisotropic pseudo-Jahn Teller vibronic interaction in the polaron formation [173] of these materials with the most recent results pointing out the role of a non-euclidean hyperbolic space (see Figure 7) for the filamentary network at the interfaces of striped puddles in high temperature superconductivity [81,174,175].
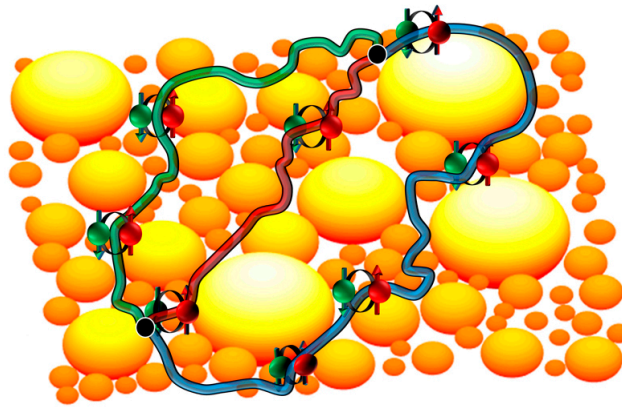
Figure 7. Superstripes landscape made of nanoscale striped puddles with a power law size distribution where the pathways of interface superconductivity connecting two points (where superconducting pairs shown in the figure) can be mapped to a hyperbolic space [81,154,174,175] providing a case of supersolid [39,94] driven by strain and doping [151,152] near a critical point of a Lifshitz transition and of large zero point lattice fluctuations [150,154,156].

5. Conclusions

Let us stress that recently discovered superconductivity in bilayer twisted graphene possibly also corresponds to the regime of BCS-BEC crossover between local and extended pairs in the d-wave channel (similarly to underdoped cuprates), but with anomalous chiral superconductivity of $d + id$ type [176] which is in agreement with the phase diagram for idealized bilayer graphene in AB modification at low doping levels [20,22,23]. The discovery of superconductivity in graphene with many properties resembling the cuprates helps the authors to build the bridge between low temperature topological superconductors based on graphene [176] and bismuth [177–179] and vanadium oxides [180–183] which are very promising for superconducting nanoelectronics and quantum calculations (for creation of topologically protected qubits). The band structure calculations and recent experimental results show the evidence for multigap superconductivity in pressurized H_3S hydrides, as well as in the recently discovered high-temperature superconductor LaH_{10} [84–86] where the superconducting dome occurs around the Lifshitz transition driven by pressure. Here the key role of Majorana exchange interaction driving the Fano shape resonance involve the new appearing small Fermi surface spots with strong pairing interactions where a strongly interacting set of states in the generalized strong-coupling approach predicted by the model of hydrogen bonds [184] is very important for hydrogen containing compounds. The evidence of shape resonance involving multiple sets of electronic states in the strong coupling regimes has been stimulating a renewed interest to doped copper perovskites where the Hubbard models, including multiple components showing the coexistence of coherent Landau quasiparticles, incoherent states and stripe order with nondispersive quasiparticles close to the Fermi energy [185,186]. Finally the physics of XXI century is reaching a universal understanding of the emergence of quantum coherence of high temperature which could be manipulated by controlling the formation of hyperbolic quantum geometries in a nanoscale phase separation superstripes scenario (see Figure 7) with interacting networks of multiple components [81,154,174,175,187] by self-organization of local structural tilts [170], the polaronic interaction [188], the zero point motion [74–76] and the mobile dopants [162,189], controlled by anisotropic strain [152,158,188] in quantum complex materials which can be observed by novel methods using a scanning sub-micron x-ray beam of focused synchrotron radiation [162].

In conclusion the maximum superconducting critical temperature has been seen to be reached at near a Lifhsitz transition with a quantum condensate in the new appearing small Fermi surface is in the BCS-BEC crossover predicted since 1996 [144–148] was first verified in MgB_2 in 2001 [190–193]. The key role of Feshbach resonance driven by Majorana exchange interaction to stabilize the quantum condensates was later confirmed also by the realization of a quasi-pure BEC condensate in fermionic ultracold gases driven by Feshbach resonance [194] the physical properties of a quantum condensate

in the BCS-BEC crossover in a single band case has been discussed for the case of ultracold gases [195]. Following the evidence for the experimental realization of the transition of Feshbach resonances in ultracold fermionic gases from negative to positive scattering length [196] in the regime of superconducting Fano shape resonances as in magnesium diboride [155–157], the theoretical interest focused in the BCS-BEC crossover first for a single electronic component [197] and recently for two electronic components [196].

Author Contributions: The authors contribute equally to the conceptualization, original draft preparation, review and editing, methodology and investigation while preparing the article.

Conflicts of Interest: The authors declare no conflict of interest.

References

1. Bednorz, J.G.; Müller, K.A. Possible high Tc superconductivity in the Ba− La− Cu− O system. *Zeitschrift für Physik B Condens. Matt.* **1986**, *64*, 189–193. [CrossRef]

2. Bednorz, J.G.; Müller, K.A. Perovskite-type oxides—the new approach to high-Tc superconductivity. *Rev. Modern Phys.* **1988**, *60*, 585. [CrossRef]

3. Anderson, P.W. The resonating valence bond state in La2CuO4 and superconductivity. *Science* **1987**, *235*, 1196–1198. [CrossRef] [PubMed]

4. Schrieffer, J.R.; Wen, X.G.; Zhang, S.C. Dynamic spin fluctuations and the bag mechanism of high-Tc superconductivity. *Phys. Rev. B* **1989**, *39*, 11663. [CrossRef]

5. Kampf, A.; Schrieffer, J.R. Pseudogaps and the spin-bag approach to high-Tc superconductivity. *Phys. Rev. B* **1990**, *41*, 6399–6408. [CrossRef]

6. Anderson, P.W.; Schrieffer, R. A dialogue on the theory of high Tc. *Phys. Today* **1991**, *44*, 54–61. [CrossRef]

7. Scalapino, D.J.; Loh Jr, E.; Hirsch, J.E. D-wave pairing near a spin-density-wave instability. *Phys. Rev. B* **1986**, *34*, 8190. [CrossRef]

8. Miyake, K.; Schmitt-Rink, S.; Varma, C.M. Spin-fluctuation-mediated even-parity pairing in heavy-fermion superconductors. *Phys. Rev. B* **1986**, *34*, 6554. [CrossRef]

9. Fukuyama, H.; Hasegawa, Y.; Narikiyo, O. Two-Dimensional Hubbard Model at Low Electron Density. *J. Phys. Soc. Jpn* **1991**, *60*, 2013–2030. [CrossRef]

10. Zhang, F.C.; Rice, T.M. Effective Hamiltonian for the superconducting Cu oxides. *Phys. Rev. B* **1988**, *37*, 3759. [CrossRef]

11. Laughlin, R.B. Superconducting ground state of noninteracting particles obeying fractional statistics. *Phys. Rev. Lett.* **1988**, *60*, 2677–2680. [CrossRef] [PubMed]

12. Lee, P.A.; Nagaosa, N. Gauge theory of the normal state of high-T c superconductors. *Phys. Rev. B* **1992**, *46*, 5621. [CrossRef]

13. Varma, C.M.; Littlewood, P.B.; Schmitt-Rink, S.; Abrahams, E.; Ruckenstein, A.E. Phenomenology of the normal state of Cu-O high-temperature superconductors. *Phys. Rev. Lett.* **1989**, *63*, 1996. [CrossRef] [PubMed]

14. Bianconi, A.; Saini, N.L. *Stripes and Related Phenomena*; Springer Science Business Media: Berlin, Germany, 2001.

15. Leggett, T. Superconducting thoughts meet sceptical resistance. *Phys. World* **1997**, *10*, 51. [CrossRef]

16. Wollman, D.A.; Van Harlingen, D.J.; Lee, W.C.; Ginsberg, D.M.; Leggett, A.J. Experimental determination of the superconducting pairing state in YBCO from the phase coherence of YBCO-Pb dc SQUIDs. *Phys. Rev. Lett.* **1993**, *71*, 2134. [CrossRef]

17. Kagan, M.Y.; Chubukov, A.V. Possibility of a superfluid transition in a slightly nonideal Fermi gas with repulsion. *JETP Lett.* **1988**, *47*, 614–617.

18. Baranov, M.A.; Kagan, M.Y. D-wave pairing in the two-dimensional Hubbard model with low filling. *Zeitschrift für Physik B Condens. Matt.* **1992**, *86*, 237–239. [CrossRef]

19. Baranov, M.A.; Chubukov, A.V.; Kagan, Y.M. Superconductivity and superfluidity in fermi systems with repulsive interactions. *Int. J. Modern Phys. B* **1992**, *6*, 2471–2497. [CrossRef]

20. Kagan, M.Y.; Mitskan, V.A.; Korovushkin, M.M. Anomalous superconductivity and superfluidity in repulsive fermion systems. *Physics-Uspekhi* **2015**, *58*, 733. [CrossRef]

21. Kagan, M.Y. Unconventional superconductivity in low density electron systems and conventional superconductivity in hydrogen metallic alloys. *JETP Lett.* **2016**, *103*, 728–738. [CrossRef]

22. Kagan, M.Y.; Mitskan, V.A.; Korovushkin, M.M. Phase diagram of the Kohn-Luttinger superconducting state for bilayer graphene. *Eur. Phys. J. B* **2015**, *88*, 157. [CrossRef]

23. Kagan, M.Y.; Val'kov, V.V.; Mitskan, V.A.; Korovushkin, M.M. The Kohn–Luttinger superconductivity in idealized doped graphene. *Solid State Commun.* **2014**, *188*, 61–66. [CrossRef]

24. Kagan, M.Y.; Val'kov, V.V.; Mitskan, V.A.; Korovushkin, M.M. The Kohn-Luttinger effect and anomalous pairing in new superconducting systems and graphene. *JETP* **2014**, *118*, 995–1011. [CrossRef]

25. Kohn, W.; Luttinger, J.M. New mechanism for superconductivity. *Phys. Rev. Lett.* **1965**, *15*, 524. [CrossRef]

26. Fay, D.; Layzer, A. Superfluidity of low-density fermion systems. *Phys. Rev. Lett.* **1968**, *20*, 187. [CrossRef]

27. Galitskii, V.M. The energy spectrum of a non-ideal Fermi gas. *Soviet Phys. JETP-USSR* **1958**, *7*, 104–112.

28. Hubbard, J. Electron correlations in narrow energy bands. Proceedings of the Royal Society of London. Series A. *Math. Phys. Sci.* **1963**, *276*, 238–257.

29. Shubin, S.; Wonsovsky, S. Zur Elektronentheorie der Metalle. *Z. Sow. Phys* **1935**, *7*, 10.

30. Shubin, S.P.; Vonsovskii, S.V. On the Electron Theory of Metals, II. *Sow. Phys.* **1936**, *10*, 348.

31. Kagan, M.Y.; Chubukov, A.V. Increase in superfluid transition temperature in polarized Fermi gas with repulsion. *JETP Lett.* **1989**, *50*, 517–520.

32. Kagan, M.Y. Strong Tc enhancement in the two-dimensional two-band Hubbard model with low filling. *Phys. Lett. A* **1991**, *152*, 303–305. [CrossRef]

33. Baranov, M.A.; Kagan, M.Y. Superconductivity in a low-density two-band model with a repulsive interaction: Extended analysis. *J. Exp. Theor. Phys.* **1992**, *75*, 165–171.

34. Kagan, M.Y. Fermi-gas approach to the problem of superfluidity in three-and two-dimensional solutions of 3He in 4He. *Physics-Uspekhi* **1994**, *37*, 69. [CrossRef]

35. Baranov, M.A.; Kagan, Y.; Kagan, M.Y. On the possibility of a superfluid transition in a Fermi gas of neutral particles at ultralow temperatures. *JETP Lett.* **1996**, *64*, 301–304. [CrossRef]

36. Kagan, M.Y.; Val'kov, V.V. Anomalous resistivity and the origin of the heavy mass in the two-band model with one narrow band. *JETP* **2011**, *113*, 156. [CrossRef]

37. Kagan, M.Y.; Val'kov, V.V. Anomalous resistivity and superconductivity in the two-band Hubbard model with one narrow band. *Low Temper. Phys.* **2011**, *37*, 69–82. [CrossRef]

38. Kagan, M.Y.; Rice, T.M. Superconductivity in the two-dimensional tJ model at low electron density. *J. Phys. Condens. Matt.* **1994**, *6*, 3771. [CrossRef]

39. Yu Kagan, M. *Modern Trends in Superconductivity and Superfluidity, Lecture Notes in Physics*; Springer: Berlin, Germany, 2013.

40. Plakida, N.M. Antiferromagnetic exchange mechanism of superconductivity in cuprates. *J. Exp. Theor. Phys. Lett.* **2001**, *74*, 36–40. [CrossRef]

41. Plakida, N.M.; Anton, L.; Adam, S.; Adam, G. Exchange and spin-fluctuation mechanisms of superconductivity in cuprates. *JETP* **2003**, *97*, 331. [CrossRef]

42. Ginzburg, V.L. On superconductivity and superfluidity (what I have and have not managed to do), as well as on the 'physical minimum' at the beginning of the XXI century (December 8, 2003). *Physics-Uspekhi* **2004**, *47*, 1155. [CrossRef]

43. Plakida, N.M.; Aksenov, V.L.; Drechsler, S.L. Anharmonic Model for High-Tc Superconductors. *Europhys. Lett.* **1987**, *4*, 1309. [CrossRef]

44. Dzyaloshinskii, I.E. Maximal increase of the superconducting transition temperature due to the presence of van't Hoff singularities. *JETP Lett.* **1988**, *46*, 118.

45. Izyumov, Y.A. The t-J model for strongly correlated electrons. *Uspekhi Fizicheskikh Nauk* **1997**, *167*, 465–498. [CrossRef]

46. Kozlov, A.I. D-wave pairing in the two-dimensional Fermi-liquid with repulsion. *Superconduct. Phys. Chem. Eng.* **1989**, *2*, 64. (in Russian).

47. Wiegmann, P. Topological superconductivity. *Prog. Theor. Phys. Suppl.* **1992**, *107*, 243–279. [CrossRef]

48. Ioffe, L.B.; Larkin, A.I. Two-dimensional Hubbard model with strong electron repulsion. *Phys. Rev. B* **1988**, *37*, 5730. [CrossRef]

49. Ovchinnikov, S.G. Quasiparticles in strongly correlated electron systems in copper oxides. *Physics-Uspekhi* **1997**, *40*, 993. [CrossRef]

50. Babichenko, V.S.; Kagan, Y. s pairing as a result of antiferromagnetic fluctuations in a high-T_c superconductor. *Jetp Letters c/c of Pis'ma V Zhurnal Eksperimental'noi Teoreticheskoi Fiziki* **1992**, *56*, 303.

51. Balatsky, A.; Abrahams, E. New class of singlet superconductors which break the time reversal and parity. *Phys. Rev. B* **1992**, *45*, 13125. [CrossRef]

52. Nagaev, E.L. Phase separation in high-temperature superconductors and related magnetic materials. *Uspekhi Fizicheskikh Nauk* **1995**, *165*, 529–554. [CrossRef]

53. Khodel, V.A.; Shaginyan, V.R. Superfluidity in system with fermion condensate. *JETP Lett.* **1990**, *51*, 553.

54. Belyavsky, V.I.; Kopaev, Y.V. Biordered superconductivity and strong pseudogap state. *Phys. Rev. B* **2007**, *76*, 214506. [CrossRef]

55. Heikkilä, T.T.; Kopnin, N.B.; Volovik, G.E. Flat bands in topological media. *JETP Lett.* **2011**, *94*, 233. [CrossRef]

56. Pudalov, V.M.; Omel'yanovskii, O.E.; Khlybov, E.P.; Sadakov, A.V.; El'tsev, Y.F.; Mitsen, K.V.; Dormidontov, A.S. VL Ginzburg and the development of experimental work on high-temperature superconductivity at LPI:'iron superconductors'. *Physics-Uspekhi* **2011**, *54*, 648. [CrossRef]

57. Gor'kov, L.P. Developing BCS Ideas in the Former Soviet Union. In *BCS: 50 Years, Cooper, L.N and Feldman, D edit*; World Scientific: Singapore, 2011; pp. 107–126.

58. Sadovsky, M.V. Electron-phonon coupling in Eliashberg-McMillan theory beyond adiabatic approximation. *JETP* **2019**, *128*, 455–463. [CrossRef]

59. Bardeen, J.; Cooper, L.N.; Schrieffer, J.R. Theory of superconductivity. *Phys. Rev.* **1957**, *108*, 1175. [CrossRef]

60. Leggett, A.J. Cooper pairing in spin-polarized Fermi systems. *Le Journal de Physique Colloques* **1980**, *41*, C7–C19. [CrossRef]

61. Nozieres, P.; Schmitt-Rink, S. Bose condensation in an attractive fermion gas: From weak to strong coupling superconductivity. *J. Low Temper. Phys.* **1985**, *59*, 195–211. [CrossRef]

62. Landau, L.D. The Theory of a Fermi Liquid. *JETP* **1956**, *3*, 920.

63. Landau, L.D. Oscillations in a Fermi Liquid. *JETP* **1957**, *5*, 101.

64. Anderson, P.W. Luttinger-liquid behavior of the normal metallic state of the 2D Hubbard model. *Phys. Rev. Lett.* **1990**, *64*, 1839. [CrossRef] [PubMed]

65. Fetter, A.L.; Hanna, C.B.; Laughlin, R.B. Random-phase approximation in the fractional-statistics gas. *Phys. Rev. B* **1989**, *39*, 9679. [CrossRef]

66. Wen, X.G.; Lee, P.A. Theory of underdoped cuprates. *Phys. Rev. Lett.* **1996**, *76*, 503. [CrossRef] [PubMed]

67. Zhang, S.C. A unified theory based on SO (5) symmetry of superconductivity and antiferromagnetism. *Science* **1997**, *275*, 1089–1096. [CrossRef]

68. Wang, Y.; Ma, Y. Perspective: Crystal structure prediction at high pressures. *J. Chem. Phys.* **2014**, *140*, 040901. [CrossRef] [PubMed]

69. Duan, D.; Liu, Y.; Tian, F.; Li, D.; Huang, X.; Zhao, Z.; Cui, T. Pressure-induced metallization of dense $(H_2S)_2H_2$ with high-T c superconductivity. *Sci. Rep.* **2014**, *4*, 6968. [CrossRef] [PubMed]

70. Drozdov, A.P.; Eremets, M.I.; Troyan, I.A.; Ksenofontov, V.; Shylin, S.I. Conventional superconductivity at 203 kelvin at high pressures in the sulfur hydride system. *Nature* **2015**, *525*, 73. [CrossRef]

71. Schrieffer, J.R. *Theory of Superconductivity*; W.A. Benjamin: Reading, MA, USA, 1964.

72. Migdal, A.B. Interaction between Electrons and Lattice Vibrations in a Normal Metal. *JETP* **1958**, *7*, 996.

73. Eliashberg, G.M. Interactions between Electrons and Lattice Vibrations in a Superconductor. *JETP* **1960**, *11*, 696.

74. Bianconi, A.; Jarlborg, T. Lifshitz transitions and zero point lattice fluctuations in sulfur hydride showing near room temperature superconductivity. *Novel Superconduct. Mater.* **2015**, *1*, 37–49. [CrossRef]

75. Bianconi, A.; Jarlborg, T. Superconductivity above the lowest Earth temperature in pressurized sulfur hydride. *EPL* **2015**, *112*, 37001. [CrossRef]

76. Jarlborg, T.; Bianconi, A. Breakdown of the Migdal approximation at Lifshitz transitions with giant zero-point motion in the H_3S superconductor. *Sci. Rep.* **2016**, *6*, 24816. [CrossRef]

77. Mazziotti, M.V.; Valletta, A.; Campi, G.; Innocenti, D.; Perali, A.; Bianconi, A. Possible Fano resonance for high-Tc multi-gap superconductivity in p-Terphenyl doped by K at the Lifshitz transition. *EPL* **2017**, *118*, 37003. [CrossRef]

78. Bianconi, A.; Poccia, N.; Sboychakov, A.O.; Rakhmanov, A.L.; Kugel, K.I. Intrinsic arrested nanoscale phase separation near a topological Lifshitz transition in strongly correlated two-band metals. *Superconduc. Sci. Technol.* **2015**, *28*, 024005. [CrossRef]

79. Bussmann-Holder, A.; Köhler, J.; Simon, A.; Whangbo, M.H.; Bianconi, A.; Perali, A. The road map toward Room-Temperature superconductivity: Manipulating different pairing channels in systems composed of multiple electronic components. *Condens. Matt.* **2017**, *2*, 24. [CrossRef]

80. Bianconi, A.; Innocenti, D.; Valletta, A.; Perali, A. Shape Resonances in superconducting gaps in a 2DEG at oxide-oxide interface. *J. Phys. Conf. Series* **2014**, *529*, 012007. [CrossRef]

81. Campi, G.; Bianconi, A.; Poccia, N.; Bianconi, G.; Barba, L.; Arrighetti, G.; Burghammer, M. Inhomogeneity of charge-density-wave order and quenched disorder in a high-T c superconductor. *Nature* **2015**, *525*, 359. [CrossRef]

82. Duan, D.; Yu, H.; Xie, H.; Cui, T. Ab Initio Approach and Its Impact on Superconductivity. *J. Superconduct. Novel Magnet.* **2019**, *32*, 53–60. [CrossRef]

83. Mozaffari, S.; Sun, D.; Minkov, V.S.; Knyazev, D.; Betts, J.B.; Einaga, M.; Balakirev, F.F. Superconducting Phase-Diagram of H_3S under High Magnetic Fields. *arXiv* **2019**, arXiv:1901.11208.

84. Somayazulu, M.; Ahart, M.; Mishra, A.K.; Geballe, Z.M.; Baldini, M.; Meng, Y.; Hemley, R.J. Evidence for superconductivity above 260 K in lanthanum superhydride at megabar pressures. *Phys. Rev. Lett.* **2019**, *122*, 027001. [CrossRef]

85. Drozdov, A.P.; Kong, P.P.; Minkov, V.S.; Besedin, S.P.; Kuzovnikov, M.A.; Mozaffari, S.; Greenberg, E. Superconductivity at 250 K in lanthanum hydride under high pressures. *Nature* **2019**, *569*, 528. [CrossRef] [PubMed]

86. Zurek, E.; Bi, T. High-temperature superconductivity in alkaline and rare earth polyhydrides at high pressure: A theoretical perspective. *J. Chem. Phys.* **2019**, *150*, 050901. [CrossRef] [PubMed]

87. Ashcroft, N.W. Metallic hydrogen: A high-temperature superconductor? *Phys. Rev. Lett.* **1968**, *21*, 1748. [CrossRef]

88. Ashcroft, N.W. Hydrogen dominant metallic alloys: high temperature superconductors? *Phys. Rev. Lett.* **2004**, *92*, 187002. [CrossRef] [PubMed]

89. Brovman, E.G.; Kagan, Y.; Kholas, A. Structure of metallic hydrogen at zero pressure. *JETP* **1972**, *34*, 1300–1315.

90. Brovman, E.G.; Kagan, Y.; Kholas, A.; Pushkarev, V.V. Role of electron-electron interaction in the formation of a metastable state of metallic hydrogen. *JETP Lett.* **1973**, *18*, 160.

91. Andreev, A.F.; Kagan, M. Hydrodynamics of a rotating superfluid liquid. *JETP* **1984**, *59*, 318.

92. Abrikosov, A.A. On the magnetic properties of superconductors of the second group. *JETP* **1957**, *5*, 1174–1182.

93. Andreev, A.F.; Lifshits, I.M. Quantum theory of defects in crystals. *JETP* **1969**, *29*, 1107.

94. Kim, E.; Chan, M.H.W. Observation of superflow in solid helium. *Science* **2004**, *305*, 1941–1944. [CrossRef]

95. Kudryashov, N.A.; Kutukov, A.A.; Mazur, E.A. Critical temperature of metallic hydrogen sulfide at 225 GPa pressure. *J. Exp. Theor. Phys.* **2017**, *124*, 143–150. [CrossRef]

96. Turlapov, A.V.; Kagan, M.Y. Fermi-to-Bose crossover in a trapped quasi-2D gas of fermionic atoms. *J. Phys. Condens. Matt.* **2017**, *29*, 383004. [CrossRef] [PubMed]

97. Kagan, M.Y.; Efremov, D.V. Two-particle pairing and phase separation in a two-dimensional Bose gas with one or two sorts of bosons. *Phys. Rev. B* **2002**, *65*, 195103. [CrossRef]

98. Bardeen, J.; Baym, G.; Pines, D. Effective Interaction of He3 Atoms in Dilute Solutions of He3 in He4 at Low Temperatures. *Phys. Rev.* **1967**, *156*, 207. [CrossRef]

99. Bashkin, E.P.; Meyerovich, A.E. 3He-4He quantum solutions. *Adv. Phys.* **1981**, *30*, 1–92. [CrossRef]

100. Van de Haar, P.G.; Frossati, G.; Bedell, K.S. (Enhancedp-wave pairing in polarized 3 He-4 He mixtures. *J. Low Temper. Phys.* **1989**, *77*, 35–59. [CrossRef]

101. Modugno, G.; Roati, G.; Riboli, F.; Ferlaino, F.; Brecha, R.J.; Inguscio, M. Collapse of a degenerate Fermi gas. *Science* **2002**, *297*, 2240–2243. [CrossRef]

102. Efremov, D.V.; Viverit, L. p-wave Cooper pairing of fermions in mixtures of dilute Fermi and Bose gases. *Phys. Rev. B* **2002**, *65*, 134519. [CrossRef]

103. Kagan, M.Y.; Brodsky, I.V.; Efremov, D.V.; Klaptsov, A.V. Composite fermions, trios, and quartets in a Fermi-Bose mixture. *Phys. Rev. A* **2004**, *70*, 023607. [CrossRef]

104. Feshbach, H. A unified theory of nuclear reactions. II. *An. Phys.* **1962**, *19*, 287–313. [CrossRef]

105. Gurarie, V.; Radzihovsky, L. Resonantly paired fermionic superfluids. *An. Phys.* **2007**, *322*, 2–119. [CrossRef]

106. Friedberg, R.; Lee, T.D. Gap energy and long-range order in the boson-fermion model of superconductivity. *Phys. Rev. B* **1989**, *40*, 6745. [CrossRef]

107. Micnas, R.; Ranninger, J.; Robaszkiewicz, S. Superconductivity in narrow-band systems with local nonretarded attractive interactions. *Rev. Modern Phys.* **1990**, *62*, 113. [CrossRef]

108. Geshkenbein, V.B.; Ioffe, L.B.; Larkin, A.I. Superconductivity in a system with preformed pairs. *Phys. Rev. B* **1997**, *55*, 3173. [CrossRef]

109. Landau, L.D.; Ginzburg, V.L. On the theory of superconductivity. *Zh. Eksp. Teor. Fiz.* **1950**, *20*, 1064.

110. Dagotto, E.; Rice, T.M. Surprises on the way from one-to two-dimensional quantum magnets: the ladder materials. *Science* **1996**, *271*, 618–623. [CrossRef]

111. Menushenkov, A.P.; Klementev, K.V.; Kuznetsov, A.V.; Kagan, M.Y. Superconductivity in $Ba_{1-x}K_xBiO_3$: Possible scenario of spatially separated Fermi-Bose mixture. *J. Exp. Theor. Phys.* **2001**, *93*, 615–624. [CrossRef]

112. Menushenkov, A.P.; Kuznetsov, A.V.; Klementiev, K.V.; Kagan, M.Y. Fermi-Bose mixture in Ba(K)BiO3 superconducting oxide. *J. Superconduct. Novel Magnet.* **2016**, *29*, 701–705. [CrossRef]

113. Bulaevski, L.N.; Nagaev, E.L.; Khomskii, D.I. A new type of auto-localized state of a conduction electron in an antiferromagnetic semiconductor. *Sov. J. Exp. Theor. Phys.* **1968**, *27*, 836.

114. Brinkman, W.F.; Rice, T.M. Single-particle excitations in magnetic insulators. *Phys. Rev. B* **1970**, *2*, 1324. [CrossRef]

115. Kagan, M.Y.; Klaptsov, A.V.E.; Brodsky, I.Y.V.; Combescot, R.; Leyronas, X. Composite fermions and bosons in ultracold gases and in high-temperature superconductors. *Physics-Uspekhi* **2006**, *49*, 1079–1084.

116. Combescot, R.; Leyronas, X.; Kagan, M.Y. Self-consistent theory for molecular instabilities in a normal degenerate Fermi gas in the BEC-BCS crossover. *Phys. Rev. A* **2006**, *73*, 023618. [CrossRef]

117. Alexandrov, A.; Ranninger, J. Theory of bipolarons and bipolaronic bands. *Phys. Rev. B* **1981**, *23*, 1796. [CrossRef]

118. Alexandrov, A.; Ranninger, J. Bipolaronic superconductivity. *Phys. Rev. B* **1981**, *24*, 1164. [CrossRef]

119. Bogoliubov, N.N. On the theory of superfluidity. *J. Phys.* **1947**, *11*, 23.

120. Einstein, A. Quantentheorie des einatomigen idealen Gases. *SB Preuss. Akad. Wiss. phys.-math. Klasse* **1925**, *1*, 3.

121. Kashurnikov, V.A.; Prokof'ev, N.V.; Svistunov, B.V. Critical temperature shift in weakly interacting Bose gas. *Phys. Rev. Lett.* **2001**, *87*, 120402. [CrossRef]

122. Petrov, D.S.; Salomon, C.; Shlyapnikov, G.V. Scattering properties of weakly bound dimers of fermionic atoms. *Phys. Rev. A* **2005**, *71*, 012708. [CrossRef]

123. Brodsky, I.Y.V.; Klaptsov, A.V.E.; Kagan, M.Y.; Combescot, R.; Leyronas, X. Bound states of three and four resonantly interacting particles. *J. Exp. Theor. Phys. Lett.* **2005**, *82*, 273–278. [CrossRef]

124. Landau, L.D.; Lifshitz, E.M. *Statistical Physics, Part 1: Volume 5*; Butterworth-Heinemann: Oxford, UK, 1980.

125. Kagan, M.Y.; Frésard, R.; Capezzali, M.; Beck, H. One-electron spectral functions of the attractive Hubbard model for intermediate coupling. *Phys. Rev. B* **1998**, *57*, 5995. [CrossRef]

126. Kagan, M.Y.; Frésard, R.; Capezzali, M.; Beck, H. One-electron spectral functions of the attractive Hubbard model at intermediate coupling. *Phys. B Condens. Matt.* **2000**, *284*, 447–448. [CrossRef]

127. Fisher, D.S.; Hohenberg, P.C. Dilute Bose gas in two dimensions. *Physical Review B* **1988**, *37*, 4936. [CrossRef]

128. Petrov, D.S.; Baranov, M.A.; Shlyapnikov, G.V. Superfluid transition in quasi-two-dimensional Fermi gases. *Phys. Rev. A* **2003**, *67*, 031601. [CrossRef]

129. Majorana, E. Über die Kerntheorie. *Zeits.Phys. A Hadrons and Nuclei* **1933**, *82*, 137.

130. Brink, D. The story of Majorana's exchange force. *Proc. Sci.* **2006**. [CrossRef]

131. Heisenberg, W. On the structure of atomic nuclei. I. *Zeit. Phys.* **1932**, *77*, 1. [CrossRef]

132. Heisenberg, W. On the structure of atomic nuclei. III. *Zeit. Phys.* **1933**, *80*, 587. [CrossRef]

133. Arima, A.; Iachello, F. *The Interacting Boson Model*; Cambridge University Press: Cambridge, UK, 1987.

134. Iachello, F.; Van Isacker, P. *The Interacting Boson-Fermion Model*; Cambridge University Press: Cambridge, UK, 1991.

135. Iachello, F. Algebraic models of many-body systems and their dynamic symmetries and supersymmetries. *J. Phys. Conf. Series* **2019**, *1194*, 012048. [CrossRef]

136. Iachello, F. Symmetry of High-Tc Superconductors. In *Symmetry and Heterogeneity in High Temperature Superconductors*; Springer: Berlin, Germany, 2006; pp. 165–180.

137. Fano, U. Sullo spettro di assorbimento dei gas nobili presso il limite dello spettro d'arco. *Nuovo Cimento* **1935**, *12*, 154. [CrossRef]

138. Fano, U. Effects of configuration interaction on intensities and phase shifts. *Phys. Rev.* **1961**, *124*, 1866. [CrossRef]

139. Palumbo, F.; Marcelli, A.; Bianconi, A. From the pion cloud of Tomonaga to the electron pairs of Schrieffer: many body wave functions from nuclear physics to condensed matter physics. *J. Superconduct. Novel Magnet.* **2016**, *29*, 3107–3111. [CrossRef]

140. Bardsley, J.N.; Mandl, F. Resonant scattering of electrons by molecules. *Rep. Prog. Phys.* **1968**, *31*, 471. [CrossRef]

141. Bianconi, A.; Vittorini-Orgeas, A. From the Majorana Theory of "Incomplete P' Triplets" to Feshbach Resonances. *PoS* **2007**, 037. [CrossRef]

142. Bianconi, A. Ugo Fano and shape resonances. *AIP Conf. Proc.* **2003**, *652*, 13.

143. Vittorini-Orgeas, A.; Bianconi, A. From Majorana theory of atomic autoionization to Feshbach resonances in high temperature superconductors. *J. Superconduct. Novel Magnet.* **2009**, *22*, 21. [CrossRef]

144. Bianconi, A.; Missori, M. The Coupling of a Wigner Polaronic Charge Density Wave with a Fermi Liquid Arising from the Instability of a Wigner Polaron Crystal: A Possible Pairing Mechanism in High Tc Superconductors. In *Phase Separation in Cuprate Superconductors*; Springer: Berlin/Heidelberg, Germany, 1994; pp. 272–289.

145. Bianconi, A.; Missori, M. The instability of a 2D electron gas near the critical density for a Wigner polaron crystal giving the quantum state of cuprate superconductors. *Solid State Commun.* **1994**, *91*, 287–293. [CrossRef]

146. Bianconi, A. The instability close to the 2D generalized Wigner polaron crystal density: A possible pairing mechanism indicated by a key experiment. *Physica C Superconduct.* **1994**, *235*, 269–272. [CrossRef]

147. Valletta, A.; Bianconi, A.; Perali, A.; Saini, N.L. Electronic and superconducting properties of a superlattice of quantum stripes at the atomic limit. *Zeitschrift für Physik B Condens. Matt.* **1997**, *104*, 707–713. [CrossRef]

148. Bianconi, A.; Valletta, A.; Perali, A.; Saini, N.L. Superconductivity of a striped phase at the atomic limit. *Physica C Superconduct.* **1998**, *296*, 269–280. [CrossRef]

149. Perali, A.; Innocenti, D.; Valletta, A.; Bianconi, A. Anomalous isotope effect near a 2.5 Lifshitz transition in a multi-band multi-condensate superconductor made of a superlattice of stripes. *Superconduct. Sci. Technol.* **2012**, *25*, 124002. [CrossRef]

150. Bianconi, A.; Di Castro, D.; Bianconi, G.; Pifferi, A.; Saini, N.L.; Chou, F.C.; Colapietro, M. Coexistence of stripes and superconductivity: Tc amplification in a superlattice of superconducting stripes. *Physica C Superconduct.* **2000**, *341*, 1719–1722. [CrossRef]

151. Kusmartsev, F.V.; Di Castro, D.; Bianconi, G.; Bianconi, A. Transformation of strings into an inhomogeneous phase of stripes and itinerant carriers. *Phys. Lett. A* **2000**, *275*, 118–123. [CrossRef]

152. Bianconi, A.; Saini, N.L.; Agrestini, S.; Castro, D.D.; Bianconi, G. The strain quantum critical point for superstripes in the phase diagram of all cuprate perovskites. *Int. J. Modern Phys. B* **2000**, *14*, 3342–3355. [CrossRef]

153. Kagan, M.Y.; Kugel, K.I. Inhomogeneous charge distributions and phase separation in manganites. *Physics-Uspekhi* **2001**, *44*, 553. [CrossRef]

154. Bianconi, A. Superstripes. *Int. J. Modern Phys. B* **2000**, *14*, 3289–3297. [CrossRef]

155. Bianconi, A.; Di Castro, D.; Agrestini, S.; Campi, G.; Saini, N.L.; Saccone, A.; Giovannini, M. A superconductor made by a metal heterostructure at the atomic limit tuned at the shape resonance': MgB_2. *J. Phys. Condens. Matt.* **2001**, *13*, 7383. [CrossRef]

156. Bianconi, A.; Filippi, M. Feshbach shape resonances in multiband high T_c superconductors. In *Symmetry and Heterogeneity in High Temperature Superconductors*; Springer: Berlin, Germany, 2006; pp. 21–53.

157. Agrestini, S.; Metallo, C.; Filippi, M.; Simonelli, L.; Campi, G.; Sanipoli, C.; Latini, A. Substitution of Sc for Mg in MgB_2: effects on transition temperature and Kohn anomaly. *Phys. Rev. B* **2004**, *70*, 134514. [CrossRef]

158. Ricci, A.; Poccia, N.; Ciasca, G.; Fratini, M.; Bianconi, A. The microstrain-doping phase diagram of the iron pnictides: heterostructures at atomic limit. *J. Superconduct. Novel Magnet.* **2009**, *22*, 589–593. [CrossRef]

159. Caivano, R.; Fratini, M.; Poccia, N.; Ricci, A.; Puri, A.; Ren, Z.A.; Barba, L. Feshbach resonance and mesoscopic phase separation near a quantum critical point in multiband FeAs-based superconductors. *Superconduct. Sci. Technol.* **2008**, *22*, 014004. [CrossRef]

160. Innocenti, D.; Poccia, N.; Ricci, A.; Valletta, A.; Caprara, S.; Perali, A.; Bianconi, A. Resonant and crossover phenomena in a multiband superconductor: Tuning the chemical potential near a band edge. *Phys. Rev. B* **2010**, *82*, 184528. [CrossRef]

161. Bianconi, A. Quantum materials: Shape resonances in superstripes. *Nat. Phys.* **2013**, *9*, 536–537. [CrossRef]

162. Campi, G.; Bianconi, A. Evolution of Complexity in Out-of-Equilibrium Systems by Time-Resolved or Space-Resolved Synchrotron Radiation Techniques. *Condens. Matt.* **2019**, *4*, 32. [CrossRef]

163. Ricci, A.; Poccia, N.; Campi, G.; Coneri, F.; Barba, L.; Arrighetti, G.; Bianconi, A. Networks of superconducting nano-puddles in 1/8 doped YBa2Cu3O6.5+y controlled by thermal manipulation. *New J. Phys.* **2014**, *16*, 053030. [CrossRef]

164. Poccia, N.; Chorro, M.; Ricci, A.; Xu, W.; Marcelli, A.; Campi, G.; Bianconi, A. Percolative superconductivity in $La_2CuO_{4.06}$ by lattice granularity patterns with scanning micro x-ray absorption near edge structure. *Appl. Phys. Lett.* **2014**, *104*, 221903. [CrossRef]

165. Bendele, M.; Barinov, A.; Joseph, B.; Innocenti, D.; Iadecola, A.; Bianconi, A.; Hatakeda, T. Spectromicroscopy of electronic phase separation in KxFe2−ySe2 superconductor. *Sci. Rep.* **2014**, *4*, 5592. [CrossRef]

166. Ricci, A.; Poccia, N.; Campi, G.; Joseph, B.; Arrighetti, G.; Barba, L.; Takano, Y. Nanoscale phase separation in the iron chalcogenide superconductor K0.8Fe1.6Se2 as seen via scanning nanofocused x-ray diffraction. *Phys. Rev. B* **2011**, *84*, 060511. [CrossRef]

167. Ricci, A.; Poccia, N.; Joseph, B.; Innocenti, D.; Campi, G.; Zozulya, A.; Takeya, H. Direct observation of nanoscale interface phase in the superconducting chalcogenide KxFe2−ySe2 with intrinsic phase separation. *Phys. Rev. B* **2015**, *91*, 020503. [CrossRef]

168. Duan, C.; Yang, J.; Ren, Y.; Thomas, S.M.; Louca, D. Appearance of superconductivity at the vacancy order-disorder boundary in KxFe2−ySe2. *Phys. Rev. B* **2018**, *97*, 184502. [CrossRef]

169. Fratini, M.; Poccia, N.; Bianconi, A. The Feshbach resonance and nanoscale phase separation in a polaron liquid near the quantum critical point for a polaron Wigner crystal. *J. Phys. Conf. Series* **2008**, *108*, 012036. [CrossRef]

170. Gavrichkov, V.A.; Shanko, Y.; Zamkova, N.G.; Bianconi, A. Is there any hidden symmetry in the stripe structure of perovskite high temperature superconductors? *J. Phys. Chem. Lett.* **2019**, *10*, 1840. [CrossRef]

171. Bianconi, A. Shape resonances in multi-condensate granular superconductors formed by networks of nanoscale-striped puddles. *J. Phys. Conf. Series* **2013**, *449*, 012002. [CrossRef]

172. Bianconi, G. Quantum statistics in complex networks. *Phys. Rev. E* **2002**, *66*, 056123. [CrossRef] [PubMed]

173. Innocenti, D.; Ricci, A.; Poccia, N.; Campi, G.; Fratini, M.; Bianconi, A. A model for liquid-striped liquid phase separation in liquids of anisotropic polarons. *J. Superconduct. Novel Magnet.* **2009**, *22*, 529–533. [CrossRef]

174. Campi, G.; Bianconi, A. High-Temperature superconductivity in a hyperbolic geometry of complex matter from nanoscale to mesoscopic scale. *J. Superconduct. Novel Magnet.* **2016**, *29*, 627–631. [CrossRef]

175. Bianconi, G.; Rahmede, C. Emergent hyperbolic network geometry. *Sci. Rep.* **2017**, *7*, 41974. [CrossRef] [PubMed]

176. Cao, Y.; Fatemi, V.; Fang, S.; Watanabe, K.; Taniguchi, T.; Kaxiras, E.; Jarillo-Herrero, P. Unconventional superconductivity in magic-angle graphene superlattices. *Nature* **2018**, *556*, 43. [CrossRef] [PubMed]

177. Li, S.; Zhang, Q.; Ghaemi, P.; Sarachik, M.P. Evidence for mixed phases and percolation at the metal-insulator transition in two dimensions. *Phys. Rev. B* **2019**, *99*, 155302. [CrossRef]

178. Kuntsevich, A.Y.; Bryzgalov, M.A.; Prudkoglyad, V.A.; Martovitskii, V.P.; Selivanov, Y.G.; Chizhevskii, E.G. Structural distortion behind the nematic superconductivity in Sr x Bi2Se3. *New J. Phys.* **2018**, *20*, 103022. [CrossRef]

179. Volosheniuk, S.O.; Selivanov, Y.G.; Bryzgalov, M.A.; Martovitskii, V.P.; Kuntsevich, A. Y of Sr doping on structure, morphology, and transport properties of Bi 2 Se 3 epitaxial thin films. *J. Appl. Phys.* **2019**, *125*, 095103. [CrossRef]

180. Whittaker, L.; Patridge, C.J.; Banerjee, S. Microscopic and nanoscale perspective of the metal− insulator phase transitions of VO_2: some new twists to an old tale. *J. Phys. Chem. Lett.* **2011**, *2*, 745–758. [CrossRef]

181. Bianconi, A. Multiplet splitting of final-state configurations in x-ray-absorption spectrum of metal VO_2: Effect of core-hole-screening, electron correlation, and metal-insulator transition. *Phys. Rev. B* **1982**, *26*, 2741. [CrossRef]

182. Singer, A.; Ramirez, J.G.; Valmianski, I.; Cela, D.; Hua, N.; Kukreja, R.; Chollet, M. Non equilibrium phase precursors during a photoexcited insulator-to-metal transition in V_2O_3. *Phys. Rev. Lett.* **2018**, *120*, 207601. [CrossRef] [PubMed]

183. Marcelli, A.; Coreno, M.; Stredansky, M.; Xu, W.; Zou, C.; Fan, L.; Bianconi, A. Nanoscale phase separation and lattice complexity in VO_2: The metal–insulator transition investigated by XANES via Auger electron yield at the vanadium L_{23}-edge and resonant photoemission. *Condens. Matt.* **2017**, *2*, 38. [CrossRef]

184. Kaplan, D.; Imry, Y. High-temperature superconductivity using a model of hydrogen bonds. *PNAS* **2018**, *115*, 5709. [CrossRef] [PubMed]

185. Fleck, M.; Lichtenstein, A.I.; Oleś, A.M. Spectral properties and pseudogap in the stripe phases of cuprate superconductors. *Phys. Rev. B* **2001**, *64*, 134528. [CrossRef]

186. Corboz, P.; Rice, T.M.; Troyer, M. Competing states in the t-J model: Uniform d-wave state versus stripe state. *Phys. Rev. Lett.* **2014**, *113*, 046402. [CrossRef]

187. Bianconi, G.; Rahmede, C. Network geometry with flavor: from complexity to quantum geometry. *Phys. Rev. E* **2016**, *93*, 032315. [CrossRef] [PubMed]

188. Bianconi, A.; Agrestini, S.; Bianconi, G.; Di Castro, D.; Saini, N.L. A quantum phase transition driven by the electron lattice interaction gives high Tc superconductivity. *J. Alloys Compound.* **2001**, *317*, 537–541. [CrossRef]

189. Jarlborg, T.; Bianconi, A. Multiple electronic components and Lifshitz transitions by oxygen wires formation in layered cuprates and nickelates. *Condens. Matt.* **2019**, *4*, 15. [CrossRef]

190. Bauer, E.; Paul, C.; Berger, S.; Majumdar, S.; Michor, H.; Giovannini, M.; Bianconi, A. Thermal conductivity of superconducting MgB2. *J. Phys. Condens. Matt.* **2001**, *13*, L487. [CrossRef]

191. Schreck, F.; Khaykovich, L.; Corwin, K.L.; Ferrari, G.; Bourdel, T.; Cubizolles, J.; Salomon, C. Quasipure Bose-Einstein condensate immersed in a Fermi sea. *Phys. Rev. Lett.* **2001**, *87*, 080403. [CrossRef] [PubMed]

192. Di Castro, D.; Agrestini, S.; Campi, G.; Cassetta, A.; Colapietro, M.; Congeduti, A.; Nardone, M. The amplification of the superconducting Tc by combined effect of tuning of the Fermi level and the tensile micro-strain in $Al_{1−x}Mg_xB_2$. *EPL* **2002**, *58*, 278. [CrossRef]

193. Perali, A.; Pieri, P.; Strinati, G.C.; Castellani, C. Pseudogap and spectral function from superconducting fluctuations to the bosonic limit. *Phys. Rev. B* **2002**, *66*, 024510. [CrossRef]

194. Regal, C.A.; Jin, D.S. Measurement of positive and negative scattering lengths in a Fermi gas of atoms. *Phys. Rev. Lett.* **2003**, *90*, 230404. [CrossRef] [PubMed]

195. Palestini, F.; Perali, A.; Pieri, P.; Strinati, G.C. Dispersions, weights, and widths of the single-particle spectral function in the normal phase of a Fermi gas. *Phys. Rev. B* **2012**, *85*, 024517. [CrossRef]

196. Tajima, H.; Yerin, Y.; Perali, A.; Pieri, P. Enhanced critical temperature, pairing fluctuation effects, and BCS-BEC crossover in a two-band Fermi gas. *Phys. Rev. B* **2019**, *99*, 180503(R). [CrossRef]

197. Guidini, A.; Perali, A. Band-edge BCS–BEC crossover in a two-band superconductor: physical properties and detection parameters. *Superconduct. Sci. Technol.* **2014**, *2*, 124002. [CrossRef]